Molecular Cloning and Characterization of an Inner Ear–Specific Structural Protein

James G. Davis, J. Carl Oberholtzer, Frank R. Burns,* Mark I. Greene†

Molecular biological studies of the mammalian inner ear have been limited by the relatively small size of the sensory endorgans contained within. The saccular otolithic organ in teleostian fish is structurally similar to its mammalian counterpart but can contain an order of magnitude more sensory cells. The prospect of the evolutionary conservation of proteins utilized in the vertebrate inner ear and the relative abundance of teleostian saccular sensory tissue made this an attractive system for molecular biological studies. A complementary DNA obtained by differential screening of a saccular complementary DNA library was identified that encodes an inner ear–specific collagen molecule.

The hair cell–containing epithelia of the vertebrate inner ear are the sensory endorgans of the vestibular and auditory systems. Typically, a specialized, gelatinous membrane or tectorium resides over the hair cell–containing sensory epithelium. This membrane is called the cupula in the semicircular canals, the otolithic membrane in the otolithic organs, and the tectorial membrane in the cochlea. Displacements of the overlying membrane and the sensory epithelium relative to one another cause stereociliary bundle displacements that result in hair cell depolarization (*1*). This same basic structural organization applies to all of the vertebrate inner ear endorgans.

Although the inner ear endorgans share a common structural organization, biochemical efforts to study the proteins involved in endorgan function have been made difficult by the relatively small size of these structures. Despite this hindrance, studies of proteins of the sensory epithelium, in particular of the hair cell stereociliary bundles, are well advanced (*2*). In addition, detailed biochemical and immunologic analyses of the tectorins (proteins of the tectoria) have been described (*3*, *4*). These studies, combined with electrophysiologic analyses, have already provided much insight into the unique structure and physiology of the vertebrate inner ear endorgans.

Because of the constraint of limiting inner ear tissue, the teleostian fish saccular otolithic endorgan was chosen for molecular biological studies. In all vertebrates the saccular sensory endorgans share a conserved structural organization and confer sensitivity to translational acceleration and to gravity. In the fish this endorgan is also capable of detecting low-frequency sounds (*5*). The anatomical relations of the saccular sensory epithelium (macula), the associated otolithic membrane, and the otoliths of the sunfish saccular endorgan are summarized in Fig. 1. The teleostian saccular macula experiences continued growth throughout the postembryonic life of the fish resulting in the accumulation of an order of magnitude more sensory cells than in the mammalian saccule (*6*). This feature made the bluegill sunfish (*Lepomis macrochirus*) saccular macula a suitable system for the construction of inner ear complementary DNA (cDNA) libraries with abundant representation of sensory epithelium transcripts (*7*).

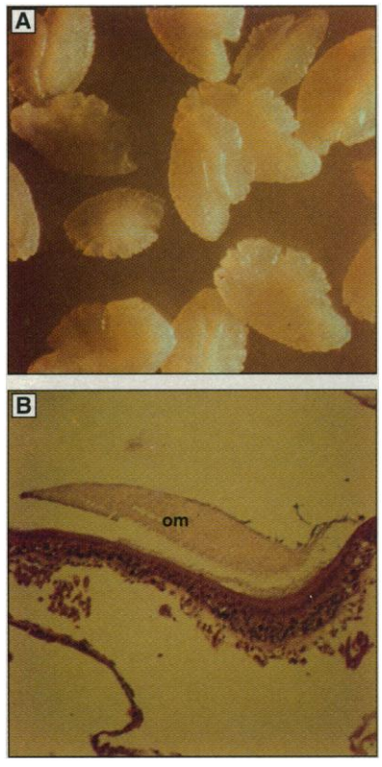

Fig. 1. Anatomy of the bluegill sunfish saccule. (**A**) Several otoliths are shown. Magnification, ×2.7. (**B**) Transverse section showing saccular macula and associated otolithic membrane (om). The otolithic membrane is detached from the macula shown. Magnification, ×67. The gelatinous otolithic membrane resides in the groove located on the medial surface of these otoliths. This membrane separates the macula from a single, calcified otolith (ear-stone) in the teleostian otolithic organs or to a collection of small calcified masses called otoconia (ear-crystals) in the mammalian saccule.

Differential screening of an oligo(dT)-primed saccular macula cDNA library with labeled saccular macula and liver cDNAs was performed (*8*) and yielded a panel of candidate saccule-specific clones. Northern (RNA) blot analysis of the first candidate saccule-specific cDNA was performed with a probe from the 3′ end of the cDNA (*9*). The transcript corresponding to this cDNA was identified as a single sequence nearly 2.0 kb in length (Fig. 2A). No transcript was detected in samples of several other sunfish tissue total RNAs, confirming the differential expression of the transcript corresponding to this cDNA. The blot was reprobed with a chicken cytoplasmic β-actin probe at high stringency to confirm RNA integrity (Fig. 2B). In addition, no detectable expression of this gene was observed in 1 μg of

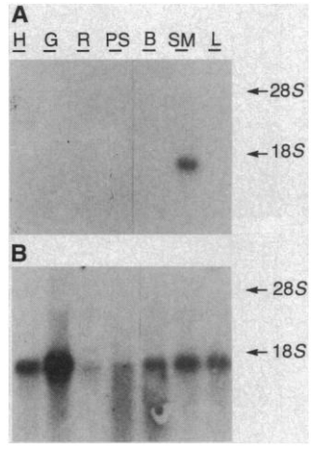

Fig. 2. RNA blot analysis of fish collagen clone. Northern analysis of 1 μg of sunfish saccular macula total RNA and 2 μg from each of the other tissue total RNAs (*9*). (**A**) The blot was probed with random-primed ^{32}P-labeled fish saccular collagen cDNA probe, washed, and exposed to film for 2 days. (**B**) The same blot was reprobed with ^{32}P-labeled chicken cytoplasmic β-actin probe, washed, and exposed to film for 6 days. Fish tissue total RNAs used are as follows: heart (H), gill (G), retina (R), pars superior portion of the inner ear (PS) (primarily the semicircular canals in this case), whole brain (B), saccular macula (SM), and liver (L). The migration positions of fish 18*S* ribosomal RNA and 28*S* ribosomal RNA are indicated.

J. G. Davis, F. R. Burns, M. I. Greene, Department of Pathology and Laboratory Medicine, University of Pennsylvania School of Medicine, Philadelphia, PA 19104, USA.
J. C. Oberholtzer, Division of Neuropathology, University of Pennsylvania School of Medicine, Philadelphia, PA 19104, USA.
*Present address: Department of Pathology, Medical College of Pennsylvania, Philadelphia, PA 19129, USA.
†To whom correspondence should be addressed.

Fig. 3. The predicted amino acid sequence and domain organization of the sunfish saccule-specific protein. The sequence of the entire sunfish sacculus-derived 1848-nucleotide cDNA was determined, and the predicted amino acid sequence of the protein encoded by the primary open reading frame is shown. This open reading frame encodes a 423–amino acid protein containing a single collagenous domain (underlined residues) flanked by small NH_2-terminal and COOH-terminal noncollagenous domains. The collagenous domain contains 70 true Gly-X-Y repeats and two minor imperfections (one Gly^{175}-X-Gly-X-Y and one Gly^{192}-X-Y-X-Y-Gly-X-Y) and has a 12% proline and an 8% lysine content. Cysteine residues located in the noncollagenous domains are circled. Potential N-linked glycosylation sites (N-X-S/T) are boxed. The first 19 amino acids of the NH_2-terminal represent a putative signal peptide. The region homologous with the collagen types VIII and X COOH-terminal noncollagenous domain is indicated with brackets. Single-letter abbreviations for the amino acid residues are as follows: A, Ala; C, Cys; D, Asp; E, Glu; F, Phe; G, Gly; H, His; I, Ile; K, Lys; L, Leu; M, Met; N, Asn; P, Pro; Q, Gln; R, Arg; S, Ser; T, Thr; V, Val; W, Trp; and Y, Tyr. X, any amino acid.

```
1                                                   50
MDAYSLSPTDSTTYSSDTFSTEFHTDAIAPPGNTPGNYTLDYNECFFNFC

                                                   100
ECCPPEKGPMGPMGERGLPGPPGERGPLGLPGEKGETGLRGPPGPAGLPG

                                                   150
ANGLNGDIGEKGDQGPVGLPGVPGIPGKPGEKGDPGLKGDKGERGFSGLK

                                                   200
GDPGERGEPGLNGTKGSIGREGPMGPGLAGTKGLKGEQGLKGECLQGEKG

                                                   250
ERGPPGLRGEMGLNGTDGVKGERGEPGPLGGKGDTGARGPPGPPGGRGMA

                                                   300
GLRGEKGLKGVRGPRGPKGPPGESVEQIRSAFSVGLFPSRSFPPPSLPVK

                                                   350
FDKVFYNGEGHWDPTLNKFNVTYPGVYLFSYHITVRNRPVRAALVVNGVR

                                                   400
KLRTRDSLYGQDIDQASNLALLHLTDGDQVWLETLRDWNGVTPAVRMTAL

                                          423
SLASCFTLTQRNLLLWKTCEGKL
```

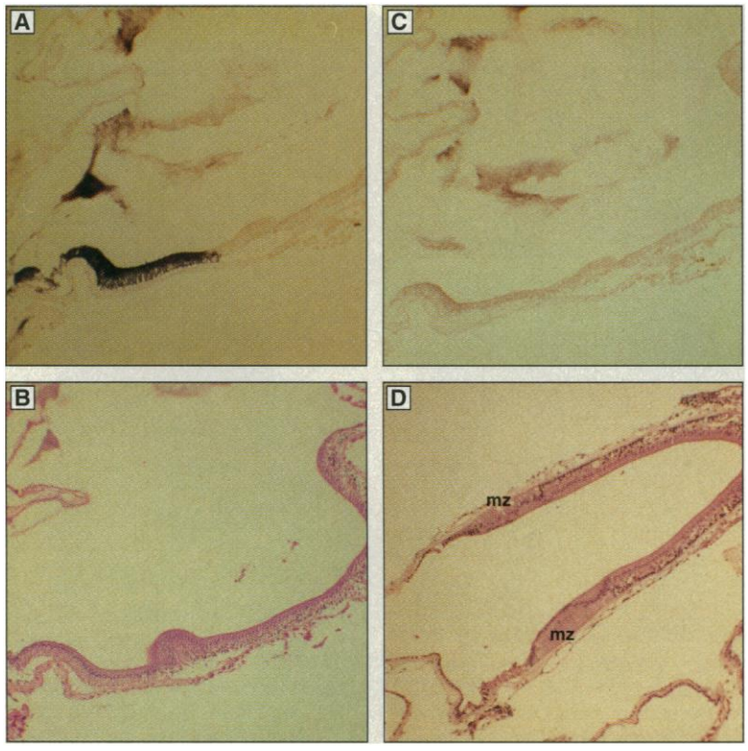

Fig. 4. Localization of saccular collagen transcripts within the sunfish saccule by nonradioactive in situ hybridization. Sunfish saccular macula sections were hybridized at high stringency with sense and antisense digoxigenin (DIG)-labeled saccular collagen riboprobes, and the resultant DIG-RNA–tissue mRNA hybrids were detected with an antibody to digoxigenin coupled to alkaline phosphatase (*14*). (**A**) Antisense probe. (**B**) Control sense probe. (**C**) Hematoxylin and eosin–stained section within 15 to 20 μm of the sections shown in (A) and (B). (**D**) Hematoxylin and eosin–stained section of additional macula cross section. The marginal zone supporting cells (mz) that reside at the edges of the epithelium are indicated. Photographs of the in situ hybridization were taken with 100-ASA Kodak color film (original magnification, ×100 for all panels).

polyadenylated [poly(A)$^+$] RNA from sunfish brain, liver, or muscle (*10*).

The full-length sequence of this saccular cDNA was determined, and the deduced amino acid sequence corresponding to the primary open reading frame (ORF) identified on this cDNA is shown (Fig. 3A). This ORF was found to encode a 423–amino acid residue protein that consists of a single, 217-residue collagenous domain flanked by a 57-residue NH_2-terminal noncollagenous domain and a 149-residue COOH-terminal noncollagenous domain. The NH_2-terminal noncollagenous domain displays no homology with any sequences reported to date. The COOH-terminal noncollagenous domain contains a region (shown between the square brackets) with high homology to the COOH-terminal noncollagenous domains of the collagen types VIII and X and, to a lesser extent, with the the soluble C1Q complement proteins (*11*). Across the 94–amino acid stretch indicated by the brackets, this region was found to contain an average of 40% identity and 56% overall homology with collagen types VIII and type X sequences (*12*) in all of the species in which these genes have been identified. This homology identifies this saccular collagen as a member of this family of short-chain collagens. The most distinguishing feature of this saccular collagen is a collagenous domain of approximately half the length of the collagenous domains in collagens type VIII and X. The presence of the conserved COOH-terminal noncollagenous domain and the lack of a lectin-binding domain in this same region distinguishes this collagen from the collectin family of short chain collagens (*13*).

Nonradioactive in situ hybridization was used to localize the expression of this gene within the sunfish saccular epithelium (*14*). Sections hybridized with antisense saccular collagen riboprobe showed that transcripts encoding this protein are localized only to the edges of the saccular epithelium (Fig. 4A), whereas sections hybridized with a control sense probe showed only light, diffuse background staining (Fig. 4B). The corresponding hematoxylin- and eosin-stained section indicated that this expression is restricted to a group of specialized secretory supporting cells (Fig. 4C) that populate the edges of the saccular epithelium. An additional histologic section is shown (Fig. 4D) in which the columnar marginal zone supporting cells are more easily identified.

Supporting cells located at the outer perimeter of the sensory surfaces of the vertebrate inner ear are thought to be involved in the formation of the tectoria associated with these epithelia (*15, 16*). These supporting cells display a secretory phenotype (*17–21*) and have been observed secreting

material that appears continuous with the corresponding tectorium (*17, 22*). Furthermore, developmental studies indicate a correlation between the appearance of these cells and the formation of the overlying tectorial structure (*16, 19, 23*). Localization of the expression of this saccular collagen gene to these secretory supporting cells suggests that this saccular collagen may be one of the structural constituents of the fish otolithic membrane. Additional support for such a role is indicated by the structural similarity of this collagen to collagen types VIII and X. These collagens form hexagonally arranged three-dimensional lattices or meshworks in which each link in the network is comprised of oligomerized collagenous regions while the nodes represent oligomers of associated noncollagenous domains. The repeating unit length (node to node distance) of these lattices is observed to be 130 nm, which corresponds to the length of the type VIII and X collagenous domains (*24*). Recent freeze-etch transmission electron microscopy studies have revealed that the amphibian otolithic membrane appears to consist, in part, of a regular hexagonally arranged structural meshwork comprised of oligomerized beaded structural units (*25*) nearly identical in appearance to those produced by collagens type VIII and X. However, the repeating unit length of the microstructural lattice of the amphibian otolithic membrane is estimated to be 40 to 60 nm (*25*), about half the length of those produced by the type VIII and X collagens. This dimension is in reasonable agreement with an estimated 60-nm length [on the basis of structural criteria set forth in (*26*)] of the collagenous domain of the saccular collagen reported here, suggesting a correspondence between the saccular collagen and this ultrastructural feature of the otolithic membrane.

On the basis of these considerations we believe that this saccular collagen is synthesized by supporting cells at the outer perimeter of the saccular macula and is secreted apically to form a microstructural matrix within the teleostian otolithic membrane (OM). This matrix would likely be hydrated by associated glycoproteins, and evidence for the existence of such glycoproteins in teleosts has been obtained in initial biochemical studies of the isolated trout OM (*4*). Although recent studies have identified certain known collagens as forming fibrillar elements within some of the tectoria (*27*), the saccular collagen reported here is clearly distinguished from these by its small size and distinct, predicted supramolecular organization.

Confirmation of this proposed structural role for the saccular collagen would designate it as a tectorin. One of the tectorins was recently cloned and encodes a glycoprotein distinct from the saccular collagen (*28*). Other tectorins were found within the avian otolithic and tectorial membranes, establishing that certain tectorins are utilized within multiple inner ear endorgan tectoria (*29*). In addition, evidence for the existence of a comparable, though not identical, microstructural framework to that observed in the amphibian OM has been observed in the mammalian OM (*30*) and tectorial membrane (*31*). It is therefore possible that this saccular collagen, or a homolog thereof, may form a microstructural framework within the gelatinous portions of the mammalian OM and TM also. Further studies of the saccular collagen may allow a more precise definition of the biomechanical properties of the inner ear tectoria and their role in sensory transduction.

REFERENCES AND NOTES

1. J. O. Pickles and D. P. Corey, *Trends Neurosci.* **15**, 254 (1992); J. T. Corwin and M. E. Warchol, *Annu. Rev. Neurosci.* **14**, 301 (1991); A. J. Hudspeth, *Nature* **341**, 397 (1989).
2. I. Thalmann *et al.*, *Arch. Otorhinolaryngol.* **226**, 123 (1980); J. C. Oberholtzer *et al.*, *Hear. Res.* **23**, 161 (1986); M. S. Tilney *et al.*, *J. Cell Biol.* **109**, 1711 (1989); D. G. Drescher *et al.*, *Brain Res.* **485**, 225 (1989); G. S. Shepherd *et al.*, *Proc. Natl. Acad. Sci. U.S.A.* **86**, 4973 (1989); G. Zajic *et al.*, *Hear. Res.* **52**, 59 (1991); P. G. Gillespie and A. J. Hudspeth, *J. Cell Biol.* **112**, 625 (1991).
3. K. P. Steel, *Acta Otolaryngol.* **89**, 27 (1980); R. Killick *et al.*, *Hear. Res.* **64**, 21 (1992).
4. K. M. Khan *et al.*, *Hear. Res.* **43**, 149 (1990).
5. A. N. Popper and R. R. Fay, *Brain Behav. Evol.* **41**, 14 (1993); C. Platt and A. Popper, in *Hearing and Sound Communication in Fishes*, W. Tavolga, A. Popper, R. Fay, Eds. (Springer-Verlag, New York, 1981).
6. J. T. Corwin, *J. Comp. Neurol.* **201**, 541 (1981); A. N. Popper and B. Hoxter, *Hear. Res.* **15**, 133 (1984).
7. Sunfish saccular macula and liver RNAs were isolated with the FastTrack mRNA isolation system (Invitrogen). Oligo(dT) and random-primed cDNA libraries were constructed from poly(A)$^+$-selected saccular macula RNA as described (J. G. Davis *et al.*, in preparation). The oligo(dT) cDNA library was constructed in λgt11 and consisted of 9.6×10^5 recombinants ranging between 0.3 and 3.5 kb in length, whereas the random-primed cDNA library was constructed in λgt10 and consisted of 1.1×10^6 recombinants ranging between 0.4 and 2.5 kb in length.
8. Differential screening was performed with ^{32}P-labeled sunfish saccular maculae and liver cDNAs prepared from poly(A)$^+$ RNAs or amplified RNAs or both. Amplified RNAs were prepared as described [R. Van Gelder *et al.*, *Proc. Natl. Acad. Sci. U.S.A.* **87**, 1663 (1990)]. First-strand cDNA synthesized with the cDNA Synthesis Plus System (Amersham) was used as template in a random-primed reaction to generate the labeled cDNA probe. Sanger dideoxy chain termination sequencing of cDNAs of interest was carried out with the Sequenase version 2.0 DNA sequencing system (U.S. Biochemical Corp.). The complete sequence for this sunfish inner ear–derived collagen was submitted to GenBank and has been assigned the accession number U17431. Nucleotide and amino acid sequence analysis was performed with MacVector 4.0 software. Homology searches were done with BLAST search programs devised by S. F. Altschul *et al.* [*J. Mol. Biol.* **215**, 403 (1990)].
9. Total RNAs were prepared by the method of guanidium isothiocyanate tissue lysis followed by acid-phenol extraction [P. Chomczynski and N. Sacchi, *Anal. Biochem.* **162**, 156 (1987)]. Northern analysis was performed with a probe specific to the last 113 amino acids of the COOH-terminal noncollagenous domain. Total RNAs were electrophoresed in a 6% formaldehyde–1% agarose gel and then were transferred and cross-linked to Zeta-Probe nylon membranes (Biorad Chemical Division, Richmond, CA). Prehybridization, hybridization, and high-stringency washes were done according to the membrane manufacturer's specifications.
10. J. G. Davis, thesis, University of Pennsylvania (1994).
11. K. B. Reid and A. J. Day, *Immunol. Today* **11**, 387 (1990); A. Brass *et al.*, *FEBS Lett.* **303**, 126 (1992).
12. N. Yamaguchi *et al.*, *J. Biol. Chem.* **266**, 4508 (1991); N. Yamaguchi *et al.*, *ibid.* **264**, 16022 (1989); Y. Ninomiya *et al.*, *ibid.* **261**, 5041 (1986); Y. Muragaki *et al.*, *ibid.* **266**, 7721 (1991); P. LuValle *et al.*, *ibid.* **263**, 18378 (1988).
13. H.-J. Hoppe and K. B. Reid, *Protein Sci.* **3**, 1143 (1994).
14. Digoxigenin (DIG)-labeled sense and antisense RNAs corresponding to a 354-nucleotide fragment (corresponding to the last 113 amino acids of the COOH-terminal noncollagenous domain and 17 nucleotides of the 3′ untranslated region) were synthesized with the Genius labeling kit (BMB, Indianapolis, IN). Similar data were also obtained with a probe specific for the 3′ untranslated region (*10*). Nonradioactive in situ hybridization was performed with the Genius nonradioactive labeling and detection system (BMB). The protocol was based in part on the manufacturer's specifications and in part on the procedure described by D. Simmons *et al.* [*J. Histotechnology* **12**, 169 (1989)]. Deparaffinized, rehydrated 5-μm sections of 10% formalin-fixed sunfish saccular maculae were treated with a solution containing 30 μg of proteinase K in 1 ml of 100 mM tris (pH 7.6), 50 mM EDTA at 37°C for 15 min. Charged sites were blocked by acetylation in 7 M acetic anhydride–30 mM triethanolamine (pH 8.0) for 20 min at room temperature. Sections were rinsed, dehydrated, vacuum dried, and incubated with 2 mg of the indicated DIG-labeled RNA per milliliter of hybridization solution [50% formamide, 5% dextran sulfate, 2× Denhardt's solution, yeast transfer RNA (250 μg/ml), 300 mM NaCl, 1 mM EDTA, 10 mM tris-HCl (pH 8.0)] for 6 hours at 50°C. The slides were rinsed and incubated with ribonuclease A (20 μg/ml), 0.5 M NaCl, 1 mM EDTA, 10 mM tris (pH 8.0) at 37°C for 20 min. High-stringency washes were performed before immunologic detection with an antibody to digoxigenin coupled to alkaline phosphatase [with X-phosphate–4-nitro blue tetrazolium chloride (NBT) substrate–based colorimetric development] according to J. Springer *et al.* [*J. Histochem. Cytochem.* **39**, 23 (1991)].
15. E. R. Lewis, E. L. Leverenz, W. S. Bialek, *The Vertebrate Inner Ear* (CRC Press, Boca Raton, FL, 1985); D. Lim, *Adv. Oto-Rhino-Laryngol.* **19**, 35 (1973); *Ann. Otol. Rhinol. Laryngol.* **82**, 23 (1973).
16. K. P. Steel, *Hear. Res.* **9**, 327 (1983).
17. M. Ciges *et al.*, *Acta Otolaryngol.* **95**, 522 (1983).
18. S. Kawamata and Y. Igarashi, *Acta Otolaryngol Suppl.* **504**, 30 (1993).
19. B. H. Sokolowski, *Scanning Electron Microsc.* **4**, 1635 (1986).
20. J. J. Prieto *et al.*, *Hear. Res.* **54**, 59 (1991).
21. J. J. Prieto *et al.*, *ibid.* **45**, 51 (1990).
22. G. Dohlman, in *Neural Mechanisms of the Auditory and Vestibular Systems*, G. L. Rasmussen and W. F. Windle, Eds. (Thomas, Springfield, IL, 1960), p. 258.
23. D. J. Lim and J. Rueda, *Acta Otolaryngol.* **110**, 224 (1990).
24. B. Kachar, M. Parakkal, J. Fex, *Hear. Res.* **45**, 179 (1990).
25. A. P. Kwan *et al.*, *J. Cell Biol.* **114**, 597 (1991); H. Sawada *et al.*, *Eur. J. Cell Biol.* **35**, 226 (1984); H. Sawada *et al.*, *J. Cell Biol.* **110**, 219 (1990); T. Schmid *et al.*, *J. Ultrastruct. Res.* **86**, 186 (1984); T. Summers *et al.*, *J. Biol. Chem.* **263**, 581 (1988).
26. A. Rich and F. Crick, *J. Mol. Biol.* **3**, 483 (1961).
27. I. Thalmann *et al.*, *Laryngoscope* **97**, 357 (1987); G. P. Richardson *et al.*, *Hear. Res.* **25**, 45 (1987); N. B. Slepecky *et al.*, *Acta Otolaryngol.* **112**, 611 (1992); N. B. Slepecky *et al.*, *Cell Tissue Res.* **267**, 413 (1992).
28. R. Killick *et al.*, abstract presented at Mechanisms of

Sensory Regeneration Conference (sponsored by the University of Virginia Office of Continuing Medical Education and by the National Institute in Deafness and other Communication Disorders), May 1994, Charlottesville, VA.
29. R. Goodyear *et al.*, *Hear. Res.* **80**, 93 (1994).
30. M. Takumida *et al.*, *Acta Otolaryngol.* **112**, 643 (1992).
31. J. Hasko and G. Richardson, *Hear. Res.* **35**, 21 (1988).
32. We thank J. Saunders, J. Eberwine, G. Massey, J. Kamholz, and D. Navaratnam for assistance and G. Richardson for helpful discussions. We also thank the M. Selzer lab for the space used to maintain the fish. Supported by grants from the Lucille P. Markey Charitable Trust to M.I.G. and from the National Institute on Deafness and other Communication Disorders (K08-DC00069) and the Pennsylvania Lions Hearing Research Foundation (GA-1307) to J.C.O. J.G.D. was supported by grants from the Lucille P. Markey Charitable Fund to M.I.G. and by training grant 5 T32 NS07064-13.

2 September 1994; accepted 2 December 1994

Prevention of Atherosclerosis in Apolipoprotein E–Deficient Mice by Bone Marrow Transplantation

MacRae F. Linton,* James B. Atkinson, Sergio Fazio

Apolipoprotein E (apoE) deficiency causes severe hyperlipidemia and atherosclerosis in humans and in gene-targeted mice. Although the majority of apoE in plasma is of hepatic origin, apoE is synthesized by a variety of cell types, including macrophages. Because macrophages derive from hematopoietic cells, bone marrow transplantation was used to examine the potential of apoE synthesized by bone marrow–derived cells to correct the hyperlipidemia and atherosclerosis caused by apoE deficiency. After transplantation of bone marrow from mice with the normal apoE gene into apoE-deficient mice, apoE was detected in serum and promoted clearance of lipoproteins and normalization of serum cholesterol levels. ApoE-deficient mice given transplants of normal bone marrow showed virtually complete protection from diet-induced atherosclerosis.

ApoE is a 34-kD glycoprotein that serves as the ligand for receptor-mediated clearance of several classes of lipoproteins, including chylomicrons, very low density lipoproteins (VLDL), and lipoprotein remnants (*1*). ApoE is thought to mediate lipoprotein clearance through its interaction with two different receptors: the LDL receptor and a putative remnant receptor (*1*), likely the LDL receptor–related protein (LRP) (*2*). Complete deficiency of apoE is a rare cause of the human genetic disorder type III hyperlipoproteinemia (HLP), a disease characterized by high serum cholesterol and triglyceride levels, accumulation of β-migrating remnant particles, and development of premature atherosclerosis (*3*). An animal model of apoE deficiency has been created by targeted inactivation of the gene locus encoding apoE in the mouse (*4*, *5*). ApoE-deficient ($apoE^{-/-}$) mice have severe hypercholesterolemia with accumulation of chylomicrons, VLDL, and remnant particles, a phenotype closely resembling that of human type III HLP. In addition, $apoE^{-/-}$ mice develop extensive aortic and coronary atherosclerosis with complex lesions that are similar in many respects to those in humans (*4*–*6*).

Studies of humans after liver transplantation have demonstrated that >90% of the apoE in plasma is synthesized by the liver (*7*), but apoE synthesis has been documented in a wide variety of tissues and cell types (*8*), including macrophages (*9*). Proposed functions for apoE synthesized by macrophages include participation in reverse cholesterol transport (*10*), promotion of local redistribution of cholesterol (*1*), and protection against atherosclerotic lesion development (*11*). Direct evidence that apoE synthesized by macrophages contributes to plasma lipoprotein clearance or influences atherosclerosis in vivo is lacking. However, apoE is secreted by mouse peritoneal macrophages in the form of lipoprotein particles in vitro (*9*), and VLDL enriched with apoE secreted by human macrophages display enhanced affinity for the LDL receptor in vitro (*12*). Because macrophages are derived from hematopoietic stem cells, we transplanted bone marrow from $apoE^{+/+}$ mice into $apoE^{-/-}$ mice to examine the capacity of apoE synthesis by bone marrow–derived cells to contribute to the clearance of plasma lipoproteins and to influence atherosclerosis in vivo.

After lethal irradiation [9 grays (Gy)] of 12 apoE-deficient mice, 6 mice received transplants of bone marrow cells from mice with the normal apoE gene ($apoE^{+/+} \rightarrow apoE^{-/-}$) and 6 control mice received marrow from apoE-deficient mice ($apoE^{-/-} \rightarrow apoE^{-/-}$) (*13*, *14*). Donor mice were derived from the ROSA β-geo 26 mice, an engineered strain that shows ubiquitous expression of the *Escherichia coli* β-galactosidase (β-Gal) from a *LacZ* gene promoter trap (*15*), providing a marker for identification of cells of donor origin by flow cytometry (*16*). Two weeks after transplantation, apoE was detectable by protein immunoblot in the serum of two out of six of the $apoE^{+/+} \rightarrow apoE^{-/-}$ mice, and by 3 weeks all six mice had detectable apoE in the serum (*17*). Ultracentrifugation analysis showed that most of the apoE in the serum of $apoE^{+/+} \rightarrow apoE^{-/-}$ mice was associated with lipoproteins, with less than 5% being recovered in the lipoprotein-free bottom fraction (*17*).

The appearance of apoE in the plasma of $apoE^{+/+} \rightarrow apoE^{-/-}$ mice was associated with dramatic changes in serum cholesterol levels (Table 1). Two weeks after transplantation, mean serum cholesterol levels were unchanged, but after 3 weeks they had decreased by almost 50%. Four weeks after transplantation, serum cholesterol levels had decreased more than 70% from baseline values, reaching values close to those in unaffected littermates (125 ± 18 mg/dl, $n = 13$). There were no significant changes in serum cholesterol in the $apoE^{-/-} \rightarrow apoE^{-/-}$ controls.

The change in the distribution of serum lipoprotein cholesterol in the $apoE^{+/+} \rightarrow apoE^{-/-}$ mice was analyzed by fast protein liquid chromatography (FPLC) analysis of serum at serial time points after bone marrow transplantation (BMT) (Fig. 1). The reduction in serum cholesterol was entirely due to a decrease in the levels of VLDL, intermediate-density lipoproteins (IDL), and LDL. The 2-week lipoprotein cholesterol profile resembled that of an apoE-deficient mouse. A marked decrease in VLDL, IDL, and LDL cholesterol was evident at the end of the third week and was more pronounced 4 weeks after transplantation (Fig. 1A). Seven weeks after transplantation (Fig. 1B), the VLDL-IDL peak in apoE-deficient serum was normalized, a small elevation in LDL remained, and HDL increased to levels similar to those of normal mice.

The efficiency of apoE in reducing serum cholesterol levels was examined by transplantation of bone marrow from mice heterozygous for the targeted disruption of the apoE allele into lethally irradiated $apoE^{-/-}$ mice ($apoE^{-/+} \rightarrow apoE^{-/-}$) and comparison of the results to those obtained in

M. F. Linton and S. Fazio, Division of Endocrinology, Department of Medicine, Vanderbilt University School of Medicine, Room AA 4206, Medical Center North, Nashville, TN 37232–2250, USA.
J. B. Atkinson, Department of Pathology, Vanderbilt University School of Medicine, Room AA 4206, Medical Center North, Nashville, TN 37232–2250, USA.
*To whom correspondence should be addressed.